

Received 6 May 2025, accepted 9 June 2025, date of publication 18 June 2025, date of current version 26 June 2025.

Digital Object Identifier 10.1109/ACCESS.2025.3580698

RESEARCH ARTICLE

An Adaptive Approach in Channel Quantization for Small Cells Based on Per-Receiver Antenna Quantization

SANJEEB SHRESTHA¹, XIAOYING KONG¹, PAUL KWAN², (Senior Member, IEEE),
AND XIAOJING HUANG³, (Senior Member, IEEE)

¹Melbourne Institute of Technology, Sydney, NSW 2000, Australia

²College of Information and Communications Technology (ICT), Central Queensland University, Brisbane, QLD 4000, Australia

³School of Electrical and Data Engineering, University of Technology Sydney, Sydney, NSW 2000, Australia

Corresponding author: Paul Kwan (w.kwan@cqu.edu.au)

This work was supported by the Open Access Journal Scheme from Central Queensland University.

ABSTRACT The widespread deployment of small cells (SCs) plays a crucial role in enhancing system capacity, coverage, and quality of service (QoS) for smart applications. However, due to the dynamic nature of user demands and the limited resources available, SCs cannot support large quantization codebooks, which are typically more suitable for macro cells (MCs) in finite rate feedback (FRF)-based multiple input single output (MISO) systems. In this paper, we propose an adaptive quantization approach for SCs that adjusts the codebook size based on the number of receiver antennas. Additionally, we address the issue of code quantization error (CQE), which arises when two distinct channels are quantized using the same code, as well as the average system error (AvgSysErr), which can increase due to elevated CQE. Our analysis shows that for SCs to achieve convergence of AvgSysErr with FRF-based MISO systems, the probability of non-unique codes in the quantization codebook must be less than $\frac{1}{N}$, where N is the number of antennas at the transmitter. Similarly, the lower bound for the non-unique code probability must be less than or equal to ε , where ε represents the difference between the non-unique code probabilities of $\frac{1}{N_1}$ and $\frac{1}{N_2}$, given $\frac{1}{N_1} > \frac{1}{N_2}$ (where N_1 and N_2 denote the number of antennas at the transmitter).

INDEX TERMS Small cells, adaptive quantization, code quantization error, finite rate feedback, average system error.

I. INTRODUCTION

Small Cells (SCs) play a crucial role in Industry 4.0 and are expected to become an integral component of Industry 5.0, 6G networks, smart cities, and the Internet of Things (IoT) [1], [2]. Applications such as cellular vehicle-to-everything (C-V2X), 6G virtual cells, private and edge networks for enterprises, and smart city infrastructure will drive the widespread deployment of SCs in the near future [3], [4], [5], [6]. Recent studies indicate that SC deployments increased by approximately 15% between 2021 and 2022, with projections estimating the number of deployments to reach 10 million

by 2030 [3]. Additionally, SCs generated approximately US\$1.1 billion in revenue in 2022, a figure expected to grow eightfold to around US\$8.2 billion by 2032 [7].

SCs utilize Access Points (APs), also known as hotspots, with limited coverage to serve user devices equipped with heterogeneous antennas, such as smart devices, HDTVs, IoT systems, and more [3]. SCs typically support varying numbers of users who can join or leave the APs randomly at any time. Due to their ability to provide ad-hoc, on-demand services, SCs are characterised by their distributed, dynamic, and dense deployments, accommodating a wide range of antenna-equipped devices. The primary goal of SCs is to enhance system coverage, capacity, and quality of service (QoS) [4], [5].

The associate editor coordinating the review of this manuscript and approving it for publication was Eyuhan Bulut¹.

In this paper, we model SCs as multi-user multiple input multiple output (MU-MIMO) systems with large number of dynamic users. We propose a per-antenna adaptive quantization approach for SCs, based on finite rate feedback (FRF), which is suitable in these dynamic environments. Specifically, we envision an adaptive and distributed codebook for SCs, given the dynamic nature of SCs. The detailed methodology for codebook generation is elaborated in the sub-sections of Section IV.

Assume that we use a large codebook for SCs similar to that used for macro cells (MCs), and powerful access points (APs) akin to base transceiver stations (BTS), to serve all users. A large codebook, however, would be ineffective for SCs, especially with users joining and leaving randomly and frequently compared to a more stable user base in MCs. A large codebook for SCs would a) quickly become disproportionate in size, and b) consume excessive bandwidth in a limited feedback system [21]. Therefore, determining an optimal codebook size that adapts to the dynamic user base in SCs and maximizes overall system resources presents an important challenge worth exploring further.

In this paper, we propose an adaptive and distributed approach that generates the quantization codebook for APs independently, based on the number of connected antenna clients. For example, consider an SC system with x' clients and a codebook size of X' at a given moment. As the number of clients changes from x' to x'' , the codebook size dynamically adjusts from X' to X'' , and vice-versa. This adaptive approach ensures that the codebook size aligns with the fluctuating number of connected users, making per-receiver antenna-based quantization essential. Moreover, since the codebooks are generated independently and randomly according to the number of receiver antennas, they exhibit a distributed nature.

However, due to the adaptive and distributed nature of codebook generation in SCs, a key challenge is the potential occurrence of non-unique quantization codes/codevectors within the codebooks. In the remaining sections, we explore the specifics, constraints, and solution strategies to address this issue and ensure the effectiveness of adaptive and distributed codebooks in SCs.

The key contributions of the paper are summarised as follows:

- We propose a per-receiver antenna quantization approach for codebook generation tailored to the densely deployed, dynamic, and distributed nature of SCs. To the best of our knowledge, this represents a novel approach.
- We introduce a threshold criterion for ensuring unique quantization codes/codevectors within the codebook. This criterion is essential for determining the appropriate codebook size and stipulates that the probability of non-unique codes must always be less than $\frac{1}{N}$, where N represents the number of antennas at the transmitter.
- The lower bound for the non-unique code probability in the adaptive quantization codebook for SCs is found to be less than or equal to ε , where ε represents the

difference between the non-unique code probabilities of $\frac{1}{N_1}$ and $\frac{1}{N_2}$, given $\frac{1}{N_1} > \frac{1}{N_2}$ (where N_1 and N_2 are the number of antennas at the transmitter). The value of ε can be used as a design parameter.

The rest of this paper is organized as follows: Section II provides a review of related work, with sub-section II-A revisiting finite rate feedback (FRF) systems and sub-section II-B discussing notations used. Section III outlines the system model of our study. Section IV delves into quantization for SCs, beginning with sub-section IV-A, which presents the per-receiver antenna quantization approach for SCs. Sub-section IV-B explores the average system error (AvgSysErr) and code quantization error (CQE) specific to SCs. Sub-section IV-C addresses the generation of quantization codebooks, while sub-section IV-D examines the relationship between AvgSysErr and non-unique code probability in SC systems. Finally, sub-section IV-E establishes the lower bound for non-unique code probability. The paper concludes with Section V, summarizing the findings and implications of our work.

II. RELATED WORK

First, we review the FRF system, which plays a crucial role in the operation of the SC systems considered in this paper.

A. REVISITING FINITE RATE FEEDBACK SYSTEM

The FRF system quantizes the channel realization using a pre-existing quantization codebook, selecting the vector that forms the smallest angle with the channel [8], [9]. The codebook consists of an N -dimensional unit-norm vectors, randomly generated with 2^B entries, where N is the number of transmit antennas and B is the number of quantization bits [8], [9], [10]. In [10], it was demonstrated that feedback beamforming remains invariant when the channel is multiplied by $e^{j\theta}$ for any θ . Additionally, [11] highlighted the effectiveness of using a small number of bits per antenna in the FRF system.

In FRF systems, real channels are quantized using a pre-existing codebook, which inevitably leads to quantization errors. Related studies [12], [13] have established upper bounds for quantization error in multiple input single output (MISO) systems. In particular, [13] concluded that in systems where the number of antennas at both the base station and mobile users is equal, the number of feedback bits, B , must increase linearly with the signal-to-noise ratio (SNR) in dB to maintain multiplexing gains equivalent to the number of transmit antennas. This, however, results in the need for a large centralized codebook. Further studies [14], [15] explore the impact of channel quantization under various conditions. In [14], a downlink channel with an FRF-MISO system is considered, where the number of antennas at mobile stations exceeds those at the base station. It was demonstrated that user diversity reduces the required number of channel state information (CSI) feedback bits to achieve target performance. Meanwhile, [15] showed that

zero-forcing dirty paper coding (ZF-DPC) with quantized feedback closely approaches the capacity of perfect CSI feedback. Additionally, [16], [17] investigate the sum-rate capacity of MIMO broadcast channels with limited feedback. In [16], the construction of M beams and the selection of users with high signal-to-interference-plus-noise ratio (SINR) is analysed, while [17] introduces per-user unitary and rate control (PU2RC) to exploit user diversity in systems with limited feedback.

Similarly, the study in [18] and the references therein examine the quantization of channel realizations using pre-designed codebooks, comparing sum-rate capacities across various scenarios. Recent findings in [19] explore single and MU-MIMO systems with finite-bit analog-to-digital converters (ADCs) and limited feedback bits, demonstrating that the number of feedback bits must increase linearly with ADC resolution to maintain performance.

The linear increase in feedback bits leads to a larger quantization codebook, which poses a significant challenge for SC systems with constrained resources. A larger codebook consumes more bandwidth on the feedback link, leaving less capacity for other users [21], [22]. The study in [21] partially addresses the relationship between feedback frequency, the number of users, and quantization bits, examining the trade-off between user diversity and accurate channel representation. In [22], the sum-rate capacity is analysed at different feedback rates using various codebooks, including Fourier, Grassmannian, and Random codebooks. The results demonstrate that Grassmannian and Random codebooks outperform the Fourier codebook in terms of sum-rate capacity. The variable length quantization (VLQ), where different binary codewords of different lengths are fed back for different channel states, compared to finite-rate CSI feedback based fixed-length quantizers (FLQS), is studied in [37]. The study takes the outage probability into account as a performance measure, and VLQ is suggested to achieve the full-CSIT outage probability performance with a finite rate when the signal-to-noise ratio (SNR) tends to infinity. However, the SNR reaching infinity is a rather ideal scenario, which may not be suitable for the SC environments. Having said that, the dynamic adaptation of the quantizer with the channel condition of the instant is an interesting proposition that we have also considered in the proposed per-antenna based quantization approach for SCs.

To the best of our knowledge, most studies on quantization codebooks have largely overlooked the potential issue of channel quantization mismatch—i.e., when two or more channel realizations are quantized using the same code. This issue in finite rate feedback (FRF) systems was identified and partially addressed in [20], which proposed a solution involving codebook rotation to preserve the uniqueness of quantization codes/codevectors and maintain the rank of the quantization matrix. However, we believe that channel quantization mismatch is a critical problem that requires deeper investigation, especially in the context of adaptive and distributed codebook generation for SCs. In these systems,

where user dynamics constantly change as users join or leave, the risk of quantization code mismatch becomes even more significant.

Overall, there is a clear need to ensure the uniqueness of channel quantization codes/codevectors for SCs. To address this, we propose a threshold criteria, which is detailed with the **Lemmas** in the following sections.

B. NOTATION

The superscript $(.)^H$ denotes the Hermitian transpose, and \mathbb{C} represents the set of complex numbers. The operators $\mathbb{E}[\cdot]$ and $\|\cdot\|$ represent the expectation and Euclidean norm, respectively. Matrices, vectors, and scalars are defined as introduced throughout the paper.

III. SYSTEM MODEL

Our system model is designed for a distributed, dynamic, and densely deployed SC environment in an urban setting, as shown in Figure 1. The circle represent the signal coverage of an MC, whereas the dotted circles represent the signal coverage of the APs. APs may serve numerous dynamic, heterogeneous users entering and leaving within their range. The intersection of the dotted circles indicates the interference region caused by adjacent APs. The term ‘heterogeneous antenna clients’ in SCs refers to devices with varying numbers of receiving antennas, such as mobile phones, laptops, HDTVs, sensors, and other smart devices.

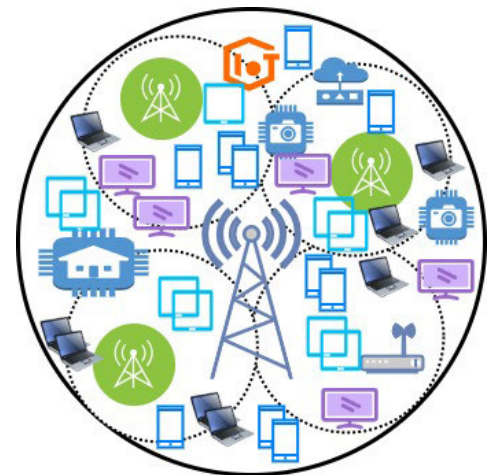


FIGURE 1. A typical small cell environment.

We characterize SCs using an MU-MIMO wireless local area network (WLAN) with K APs and users, as illustrated in Figure 2a. Each AP is equipped with N antennas, while the users have heterogeneous antenna configurations, denoted by the variable M . An enlarged view of the j th AP and its user, incorporating FRF, is shown in Figure 2b. For our analysis, we use the j th AP-user pair as the reference point.

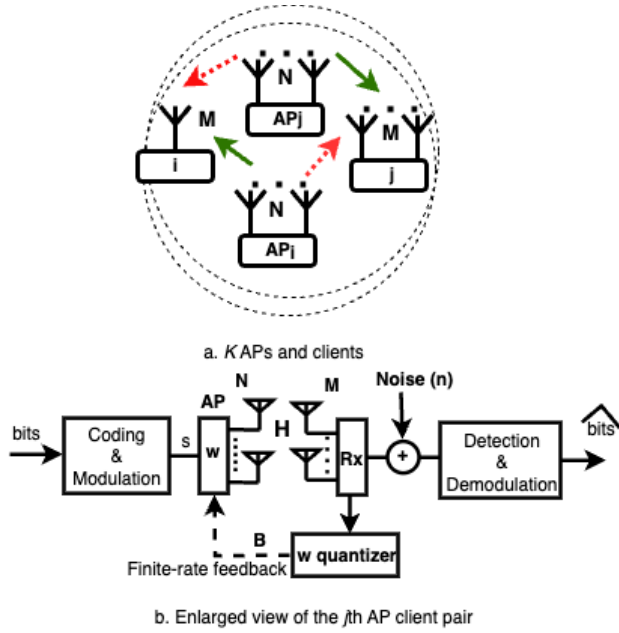


FIGURE 2. Modelling a typical small cell environment.

The received signal \mathbf{y}_j at the j th user or client is expressed as

$$\mathbf{y}_j = \mathbf{H}_{jj}^H \mathbf{v}_j s_j + \sum_{i=1, i \neq j}^K \mathbf{H}_{ij}^H \mathbf{v}_i s_i + \mathbf{n}_j. \quad (1)$$

The channels $\mathbf{H}_{jj} \in \mathbb{C}^{N \times M}$ and $\mathbf{H}_{ij} \in \mathbb{C}^{N \times M}$ follow independent and identically distributed (i.i.d.) Rayleigh fading. The beamforming vector is denoted by $\mathbf{v} \in \mathbb{C}^{N \times 1}$, while $\mathbf{n} \in \mathbb{C}^{M \times 1}$ represent the noise at the client. The noise is modelled as an independent complex Gaussian random process with variance $\sigma^2 = 1$. The scalar complex symbol intended for the j th client is s_j , with symbol power given by $\mathbb{E}[|s|^2] = P$.

Each AP serves its heterogeneous antenna clients, forming channel realizations represented by a composite matrix \mathbf{H} , where $\mathbf{H} = [\mathbf{h}_1 \mathbf{h}_2 \mathbf{h}_3 \dots \mathbf{h}_M] \in \mathbb{C}^{N \times M}$. The matrix $\mathbf{H}^H \in \mathbb{C}^{M \times N}$ corresponds to the transposed channels, with the i th row representing the channel of the i th receiver (denoted by \mathbf{h}_i^H). In the overlapping areas (of the dotted circles), the channel matrices \mathbf{H}_{ji} and \mathbf{H}_{ij} capture interference effects, where the i th and j th users experience interference from multiple transmitters in each other's range.

We normalize the channels for both desired and undesired users within the dotted circles. For instance, $\tilde{\mathbf{H}}_{jj} \triangleq \frac{\mathbf{H}_{jj}}{\|\mathbf{H}_{jj}\|^2}$, where \mathbf{H}_{jj} represents the channel from the j th transmitter to the j th receiver (i.e., the desired signal). The same normalization process is applied to the undesired channels, such as the j th transmitter to the i th receiver (i.e., the undesired signal).

For the FRF system, each column of the normalized channel matrix $\tilde{\mathbf{H}}_{jj} = [\tilde{\mathbf{h}}_1, \tilde{\mathbf{h}}_2, \dots, \tilde{\mathbf{h}}_j, \dots, \tilde{\mathbf{h}}_M]$ where $\tilde{\mathbf{h}}_j \in$

$\mathbb{C}^{N \times 1}$, is individually quantized using a codebook. The codebook is created with B' quantization bits and contains quantization vectors $\mathbf{C} \triangleq \{\mathbf{w}_1, \mathbf{w}_2, \dots, \mathbf{w}_{2^{B'}}\}$, which are selected to form the minimum angle with the channel vectors [8], [9]. Thus,

$$\hat{\mathbf{h}}_j = \arg \min_{\mathbf{w} \in \mathbf{C}} \sin^2(\angle(\tilde{\mathbf{h}}_j, \mathbf{w})), \quad (2)$$

and $\hat{\mathbf{H}} = [\hat{\mathbf{h}}_1, \hat{\mathbf{h}}_2, \dots, \hat{\mathbf{h}}_j, \dots, \hat{\mathbf{h}}_M]$.

Additionally, as we envision an adaptive and distributive per-antenna-based quantization approach for dynamic and heterogeneous users in SCs, the quantization codebook would adjust dynamically according to the number of receiving antennas at the client.

Considering the use of the downlink zeroforcing (ZF) technique, the precoding vector for client j , $\hat{\mathbf{v}}_j$, is aligned with the projection of $\tilde{\mathbf{H}}_{jj}$ onto the null space of $\{\tilde{\mathbf{H}}_{ji}\}_{i \neq j}$. We assume equal power allocation across the scheduled users, i.e., $\gamma = \frac{P}{N}$. Therefore, the SINR is given by

$$\text{SINR}_j = \frac{\gamma \|\mathbf{H}_{jj}\|^2 \|\tilde{\mathbf{H}}_{jj}^H \hat{\mathbf{v}}_j\|^2}{\sigma^2 + \sum_{i \neq j}^K \gamma \|\mathbf{H}_{ij}\|^2 \|\tilde{\mathbf{H}}_{ij}^H \hat{\mathbf{v}}_i\|^2}. \quad (3)$$

Following [31], [32], we use the expected interference constraint (IC) values $(\mathbb{E} \|\tilde{\mathbf{H}}_{ij}^H \hat{\mathbf{v}}_i\|^2, \mathbb{E} \|\tilde{\mathbf{H}}_{ji}^H \hat{\mathbf{v}}_j\|^2)$ as

$$\mathbb{E} \|\tilde{\mathbf{H}}_{ij}^H \hat{\mathbf{v}}_i\|^2 = \frac{1}{(N-1)} 2^{-\frac{B}{M(N-1)}} \quad (4)$$

and the expected quantization error as

$$\mathbb{E} [\sin^2(\angle(\tilde{\mathbf{H}}_{jj}, \hat{\mathbf{H}}_{jj}))] < 2^{-\left(\frac{B}{M(N-1)}\right)}, \forall M > 1. \quad (5)$$

IV. QUANTIZATION FOR SMALL CELLS

In this section, we discuss the quantization scheme for SCs, its benefits and constraints, and the threshold criteria to address the constraints.

A. PER-RECEIVER ANTENNA QUANTIZATION FOR SMALL CELLS

The per-receiver antenna quantization approach considers each antenna at the receiver/client, represented as $M = [M_1, M_2, \dots, M_M]$, for channel quantization. Specifically, each receiving antenna contributes equally to the total quantization bits B' . This is unlike the FRF-MISO and FRF-MIMO systems, where B' increases linearly with SNR [13].

When B' increases linearly with SNR, it forms a huge codebook with $2^{B'}$ for quantization, which may not be suitable for densely deployed, fast-changing dynamic systems like SCs. The heterogeneous antenna clients may join or leave the network at any point, rendering the huge quantization codebook ineffective in its size for quantization. Instead, we take an adaptive approach to creating a quantization codebook for SCs. The codebooks are dynamic, and they

adapt to the fast-changing heterogeneous clients' activities. In other words, the per-receiver antenna quantization approach generates or ceases the quantization codebook according to the client's changing heterogeneous antennas.

The concept of per-receiver antenna quantization was partially explored in [32], where the analytical expression for the expected quantization error is given in (4). Suppose B' represents the total number of quantization bits and M' is the number of antennas at the receiver for an SC at any given instant, then the per-receiver antenna quantization bits are denoted by $\beta = \frac{B'}{M'}$. These β quantization bits are used to independently and randomly generate 2^β quantization codes/codevectors at the APs for each receiver antenna. Consequently, as M' varies, the quantization codebook size, 2^β , also varies with the change in β . This leads to a dynamic codebook of size $C_{N \times M'}$, where C represents the quantization codebook.

To ensure maximum multiplexing gain in MU-MIMO systems, the generated quantization codebook must maintain consistency with the expected quantization error for both MU-MIMO and MISO systems. Without this conservation, using additional resources in MU-MIMO would be unjustified, as an increase in antennas should not lead to a higher error floor. Therefore, we equate the expected quantization error for both systems as

$$2^{-\left(\frac{B'}{M'(N-1)}\right)} = 2^{-\left(\frac{B}{N-1}\right)} \quad (6)$$

and hence

$$B' = M'B. \quad (7)$$

This process allows for the dynamic generation of the quantization codebook as the system evolves. The derived expression (7) aligns with the analytical result for B found in [31], where $M' = 1$ leads to $B' = B$.

The following points are noteworthy. First, there is a linear relationship between B' (the total quantization bits) and the number of receiver antennas, M' . Second, the slope of this relationship is always B , meaning: a) The optimal quantization bits B for a single antenna receiver also apply to multiple antennas, making the system scalable. This is consistent with findings in [21], where more accurate CSI feedback is shown to be critical for improving the system's sum rate,¹ b) As M' increases, the corresponding increase in B' leads to a larger set of quantization codes/codevectors generated with 2^β , and vice-versa, as illustrated in Figure 3. This dynamically updating of the codebook ensures it remains effective and adaptive to the changing nature of SCs.

Consider an example with an $N = 6$ and $M = 4$ MU-MIMO system, forming a 6×4 composite channel realizations matrix, \mathbf{H} . We take four sets of 6×1 channel realizations of \mathbf{H} into account as per the proposed per-receiver

antenna quantization approach for SCs. Each channel realization is then quantized with four independent and distributive codebooks, each generated with 2^β , where $B' = 4B$, $\beta = \frac{B'}{4} = B$.

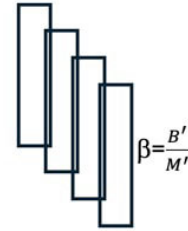


FIGURE 3. A typical case of per receiver antenna quantization with $M = 4$, where each rectangle arbitrarily represents a distributive quantization code formed with 2^β .

Illustratively, the process of code generation can be likened to rolling M independent N -sided unbiased dices (referred to as code generators). Each time these dice are rolled, the outcomes correspond to the quantization codes/codevectors needed for the channel realizations in SCs. The goal of this process is to create N -dimensional unit norm vectors that effectively quantize the channel realizations associated with the M receiving antennas. The details of the code generation process are elaborated further in Section IV, C.

The per-receiver antenna quantization scheme offers several key benefits for SC systems: a) Adaptability to dynamic SC operations: The per-receiver quantization codebook responds to the dynamic nature of SCs networks, where users frequently join or leave. Codebooks are generated only for the active receivers based on B' and M' , ensuring the codebook is always up-to-date with the current network users. b) Reduction in codebook size: This scheme significantly reduces the large quantization codebook typically seen in MISO systems, where B increases linearly with SNR. This results in a more cost-effective use of feedback bandwidth. c) Efficiency for small-cell APs: By tailoring the codebook size to the per-receiver antennas, this approach ensures an efficient and manageable codebook size for APs, perfectly aligned with the resource-constrained nature of small-cell APs.

However, since the quantization codebooks for each receiving antenna are generated independently, distributively, and randomly, there is a significant risk of duplicate codes within the codebook. The main challenge, therefore, is to minimize the probability of identical codes appearing in the quantization codebook, as this would lead to CQE.

We propose addressing CQE in SC systems through a threshold criterion designed to ensure unique codes in the quantization codebook for all channel realizations at any given moment. The details and examples of this threshold criterion are presented in Lemma 1 and Lemma 2 in Sections IV-D and IV-E, respectively. Next, we examine the impact of CQE on per-receiver antenna quantization,

¹The linear increase of B , as in (7), mirrors the concept of grouping antennas in frequency/time blocks, which then feedback more precise CSI within subsets of these coherence block.

particularly in a distributed scenario where it can accumulate and contribute to AvgSysErr.

AvgSysErr refers to the error distributed across receiver antennas at a specific instant. While multiple factors can contribute to a system error, we assume that other sources—such as (i) feedback link bandwidth and feedback frequency, ii) dynamic changes in the channel, and iii) channel estimation error—are properly mitigated. Under these conditions, AvgSysErr primarily depends on two key factors: a) quantization error and b) CQE.

The upper bound of quantization error is well-known, given the quantization bits B [12], [13], [20]. Thus, the average quantization error per receiver antenna becomes the same for both MISO and MU-MIMO systems, as shown in (7). In this context, we anticipate that CQE will be the principal contributor to AvgSysErr. The relationship between AvgSysErr and CQE is discussed in detail in the subsequent sections.

B. AVERAGE SYSTEM ERROR (AVGSYSERR) AND CODE QUANTIZATION ERROR (CQE) FOR SMALL CELLS

AvgSysErr is defined as the ratio between the total quantization error for the receiver antennas considered and the number of unique quantization codes/codevectors in the codebook at any given moment. Alternatively, it can be expressed as the per-receiver antenna quantization error

$$\text{AvgSysErr} = \frac{M' \times 2^{-\frac{B'}{M'(N-1)}}}{M_c''} \quad (8)$$

where $M' = M_c'' \times x$. M' is the number of receiving antennas considered by the system, M_c'' is the number of required unique quantization codes/codevectors in the codebook for the transmitter-receiver antenna system (i.e., $N \times M'$) at that instant, and x is a multiplier. The analytical expression of x is discussed further.

The system requires unique quantization codes/codevectors for each unique channel realization in MU-MIMO systems. If not, CQE arises, increasing the AvgSysErr, denoted as Avg' . The difference $(M' - M_c'')$ represents the number of non-unique codes in the codebook.

Given the distributive approach in codebook generation for SCs, $(M' - M_c'')$, is given by [35]

$$M' - M_c'' = M' \frac{2^{B'}}{N^{M'}} \quad (9)$$

where $\frac{2^{B'}}{N^{M'}}$ is the ratio of the number of quantization codes/codevectors, $2^{B'}$, and the number of possible outcomes, $N^{M'}$, which is also regarded as a mapping strategy of the proposed scheme, and is further illustrated in Section IV, C.

Figure 4, shows how the number of non-unique codes varies with the number of receiver antennas M , given N and B . We see that as the number of M increases the number of non-unique codes decreases with given N and B .

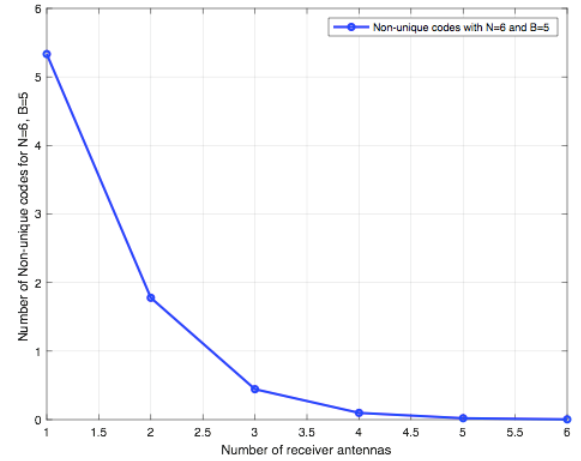


FIGURE 4. Number of Non-unique codes when $N = 6$ and $B = 5$ with varying M .

Since we know the upper bound on quantization error for SCs, $2^{-\frac{B'}{M'(N-1)}}$, CQE can be expressed as

$$\text{CQE} = (M' - M_c'') 2^{-\frac{B'}{M'(N-1)}}. \quad (10)$$

The updated system error Avg' then becomes

$$\begin{aligned} \text{Avg}' &= \text{AvgSysErr} + \text{CQE} \\ &= \frac{M' \times 2^{-\frac{B'}{M'(N-1)}}}{M_c''} + (M' - M_c'') 2^{-\frac{B'}{M'(N-1)}} \\ &= 2^{-\frac{B'}{M'(N-1)}} \left(\frac{M'}{M_c''} + (M' - M_c'') \right) \\ &= 2^{-\frac{B'}{M'(N-1)}} (x + (M' - M_c'')) \end{aligned} \quad (11)$$

where x is the multiplier that accounts for the deviation of the system from the ideal case. The multiplier x can be derived as

$$\begin{aligned} x &= \left(\frac{\text{Avg}'}{2^{-\frac{B'}{M'(N-1)}}} \right) + M_c'' - M' \\ &= \frac{\text{Avg}' - (M' - M_c'') 2^{-\frac{B'}{M'(N-1)}}}{2^{-\frac{B'}{M'(N-1)}}} \\ &= \frac{\text{Avg}' - \text{CQE}}{2^{-\frac{B'}{M'(N-1)}}}. \end{aligned} \quad (12)$$

This leads to

$$M' = \left(\left(\frac{\text{Avg}'}{2^{-\frac{B'}{M'(N-1)}}} \right) + M_c'' - M' \right) M_c''.$$

Case 1: If the required unique codes match the number of receiving antennas ($M_c'' = M'$), then $x = 1$, meaning CQE is zero and AvgSysErr is conserved.

Case 2: If $M_c'' < M'$, x increases, causing CQE to rise and thus increasing Avg' .

Case 3: If $M_c'' > M'$, x decreases, leading to a drop in CQE and Avg'.

It is noteworthy that since CQE and $2^{-\frac{B'}{M'(N-1)}}$ in (12) simply represents the rate at which x decreases, when Avg' increases, x also increases. Conversely, when Avg' decreases, x also decreases. Therefore, AvgSysErr will not be conserved for both MISO and SC systems in Cases 2 and 3. The accumulated error is given in (10).

It is important to note that Case 3 serves as a theoretical discussion for illustrative purposes. In reality, when $M_c'' > M'$, the CQE reduces to zero, as the condition $M_c'' = M'$ is already satisfied. This implies that there are sufficient quantization codes/codevectors to accommodate all channel realizations, eliminating the occurrence of code quantization errors.

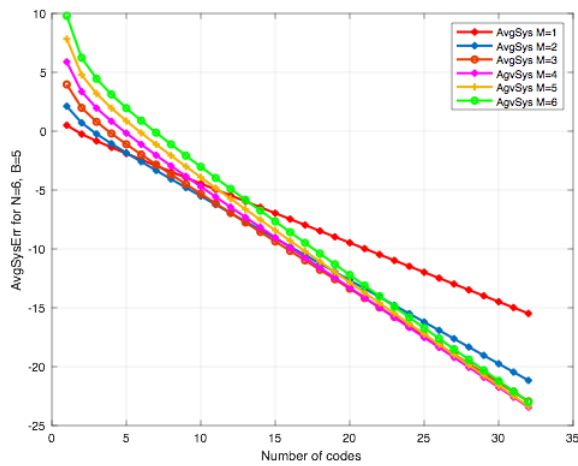


FIGURE 5. AvgSysErr vs Number of Codes in the codebook for $N = 6$, $B = 5$ and $M = 1, M = 2, M = 3, M = 4, M = 5, M = 6$.

Figure 5 illustrates the relationship between AvgSysErr and the number of quantization codes/codevectors in the codebook as in (11), for $N = 6$, $B = 5$ (which gives $2^5 = 32$ codes) and $M = 1, M = 2, M = 3, M = 4, M = 5$, and $M = 6$. The goal is to demonstrate how AvgSysErr varies with the number of quantization codes/codevectors and varying M .

We observe that Figure 5, a) effectively visualizes the three previously discussed cases, and b) demonstrates the decrement of AvgSysErr with increasing receiving antenna M , given the quantization codes/codevectors, which apparently demonstrates the advantage of distributive per-receiver antenna quantization over traditional centralized quantizations.

First, consider a scenario where the number of quantization codes/codevectors is set to $M_c'' = 5$. In Case 1, where $M_c'' = M'$, Figure 5 shows that the AvgSysErr is slightly greater than zero. This result is expected, as when $M_c'' = M'$, the AvgSysErr corresponds to $2^{-\frac{B'}{M'(N-1)}}$ for the given values of B and M' . This observation holds consistently across all combinations of B , M' and M_c'' .

In Case 2, where, $M_c'' < M'$ (e.g., $M' = 6$ and $M_c'' = 5$), Figure 5 indicates that the AvgSysErr is higher than when $M' = 5$. Conversely, in Case 3, where $M_c'' > M'$ (e.g., $M' = 4$ and $M_c'' = 5$), the figure shows that the AvgSysErr is lower than when $M' = 5$.

In Case 2, the CQE increases, leading to a corresponding increase in AvgSysErr. In contrast, in Case 3, the CQE theoretically decreases, which further reduces the AvgSysErr.

Overall, ensuring unique quantization codes/codevectors is crucial for SCs employing per-receiver antenna quantization. When multiple channel realizations are quantized using identical codes (which could come from independent, dynamic, and distributive quantization codes/codevectors), it leads to CQE, which subsequently increases the AvgSysErr.

Second, the AvgSysErr is significantly improved, up to 48 %, given $B = 5$ and $M = 2, M = 3, M = 4, M = 5$ and $M = 6$, compared to $M = 1$.

It is to be noted that when we have $M = 1$, we have a huge centralized codebook that represents the standard quantization approach used in the MISO systems where quantization codes/codevectors linearly increase with SNR. In contrast, when we have $M > 1$, the proposed pre-antenna quantization approach comes in-effect which creates an adaptive and distributive quantization codes/codevectors for SCs with the increment and decrement of M' as in (7).

Since we observe that the AvgSysErr is significantly improved when $M > 1$ compared to $M = 1$, we conclude that in terms of AvgSysErr, the proposed per-antenna quantization approach for SCs outperforms the standard centralized approach for the generation of quantization codes/codevectors.

The decrement in the AvgSysErr with the increment of M is evident as the number of non-unique quantization codes/codevectors decreases with the increment of M as in (9) and is illustrated in Figure 3. Moreover, the decrement of the non-unique quantization codes/codevectors further reduces the CQE as in (10), which further reduces AvgSysErr as in (11).

C. QUANTIZATION CODEBOOK GENERATION

Unlike MISO systems, the codebook for SCs is generated distributively, independently, and randomly based on the dynamic arrival and departure of clients. The generated codebook for SCs must account for three key factors: a) minimizing the probability of duplicate codes, thereby maximizing the likelihood of unique quantization codes/codevectors for the receiver antennas, denoted as $P(\text{Uniq}, M)$; b) ensuring a 1:1 mapping between the generated codes, 2^B , and the total number of possible code combinations, N^M , to guarantee the availability of at least one unique code; and c) considering the number of transmitter antennas, N , and receiver antennas, M , at that moment.

First, it is essential that the quantization codebook remains unique for SC systems. Given the dynamic nature of SC operations—characterised by distributed, independent, and random client interactions—duplicate quantization

codes/codevectors within the codebook can be unavoidable. The presence of identical quantization codes/codevectors leads to CQE in the system. Therefore, it is crucial to establish a minimum probability of non-unique codes, denoted as $P(\text{Non_Uniq}, M)$, as one of the key components in the codebook generation process. Details regarding the minimum $P(\text{Non_Uniq}, M)$ are provided in **Lemma 2**.

Second, the total number of quantization codes/codevectors is represented by 2^β , while the number of potential outcome combinations is given by N^M . Consequently, it is necessary to establish a mapping between the quantization codes/codevectors and the combinations of possible outcomes represented by N^M at any given moment.

Third, the number of transmitter antennas, N , and the number of receiver antennas, M , must be taken into account in SC systems at any instant, as these parameters define the composite channel matrix that requires appropriate quantization codes/codevectors.

For illustrative purposes, let's examine the quantization code requirements for an SC system with $N = 6$ and $M = 2$. This configuration produces a composite channel matrix of size 6×2 . The number of quantization codes/codevectors, represented by 2^β , must correspond to the number of possible outcome combinations given by N^M , taking into account the distributed, independent, and random generation of the quantization codes/codevectors. In this case, there are 6×6 possible outcome combinations. The probability of generating duplicate outcomes can be calculated as [33], [34]

$$P(\text{Non_Uniq}, 2) = \frac{\binom{2}{2} \times N}{N^2}. \quad (13)$$

This results in $P(\text{Non_Uniq}, 2) = \frac{1}{6}$. Thus, the total number of possible outcome combinations for $N = 6$ and $M = 2$ is given by N^M , or $6^{6 \times 6}$ possible combinations. This must map effectively to the number of quantization codes/codevectors represented by 2^β .

In scenarios where a 1:1 mapping is not achievable, a code selection mechanism may be necessary, allowing multiple codes to be used for channel quantization. The study of the code selection mechanisms where there are mappings other than 1:1 between the generated codes, 2^β , and the number of possible outcomes, N^M , is not straightforward—represents an interesting avenue for future research. However, this paper focuses primarily on the specific requirements for unique codes in channel quantization to mitigate AvgSysErr. In the recent work in [35], a null algorithm is proposed to mitigate the AvgSysErr. The efficiency of the null algorithm in mitigating CQE is analyzed with analytical expression and simulation results.

D. AVGSYSERR AND NON-UNIQUE CODE PROBABILITY FOR SC SYSTEMS

Lemma 1: *The average system error (AvgSysErr) for small cell (SC) systems remains consistent with that of the finite rate feedback (FRF) multiple input single output (MISO) system*

when the probability of generating non-unique quantization codes/codevectors is consistently less than $\frac{1}{N}$, where N represents the number of antennas at the transmitter.

Proof: Consider an $N \times M$ FRF MU-MIMO system.

Lemma 1 stipulates that the probability of generating non-unique codes in the quantization codebook must be less than $\frac{1}{N}$.

The non-unique code probability is defined as the likelihood of having identical quantization codes/codevectors within a codebook at any given moment. Formally, this is expressed as [33], [34]

$$P(\text{Non_Uniq}) = \frac{n(\text{Non_Uniq})}{n(\text{Non_Uniq} + \text{Uniq})} \quad (14)$$

where $P(\text{Uniq}) = 1 - P(\text{Non_uniq})$. Here, $P(\text{Non_Uniq})$ represents the probability of non-unique codes, $P(\text{Uniq})$ denotes the probability of unique codes, $n(\text{Non_Uniq})$ indicates the number of non-unique codes, and $n(\text{Uniq})$ is the number of unique codes.

We will examine **Lemma 1** by employing contradictory scenarios: first, when the non-unique code probability of the generated quantization codes/codevectors is a) equal to $\frac{1}{N}$, and b) greater than $\frac{1}{N}$. We will demonstrate that these contradictory arguments do not hold true. This analysis applies universally to all clients with heterogeneous antennas at the receiver. Finally, we will substantiate **Lemma 1** with an illustrative example.

Assumption 1: Let us assume that the AvgSysErr for SCs is conserved with that of the FRF MISO system when the non-unique code probability of the generated quantization codes/codevectors is equal to $\frac{1}{N}$. **Assumption 2:** Let us assume that the AvgSysErr for SCs is conserved with the FRF MISO system when the non-unique code probability of the generated quantization codes/codevectors is greater than $\frac{1}{N}$.

We begin by examining **Assumption 1**. For example, consider $N = 6$ and $M = 2$, which results in a 6×2 MU-MIMO system. This system requires at least 12 unique quantization codes/codevectors to represent 12 distinct channel realizations. Here, the non-unique code probability is $\frac{1}{6}$, given $N = 6$.

Since the quantization codes/codevectors are generated independently and randomly, for $M = 2$, we can model the process using two unbiased $N = 6$ -sided code generators to create a quantization codebook for quantizing each column of the composite channel matrix \mathbf{H} . Thus, for $M = 2$, the process independently generates $6^{6 \times 6}$ possible combinations of codes, as described earlier. From these combinations, $6^{6 \times 2}$ quantization codes/codevectors are required for the 6×2 SC system.

It is clear that, due to the independent, distributive, and random nature of code generation for SCs, two of the 12 codes—namely, c_{11} and c_{22} —may exhibit similarities. As a result, we have 10 unique codes for 12 channel realizations, which leads to $M'_c < M'$. This situation corresponds to Case 2 discussed previously. Additionally, the codebook exhibits a non-unique code probability of $\frac{1}{6}$ and a

unique code probability of $\frac{5}{6}$. Consequently, we conclude that when the non-unique code probability is $\frac{1}{N}$, the AvgSysErr of the SC system will not align with that of the FRF MISO system.

Assumption 2: Following a similar approach, let us now consider the case where the non-unique code probability is $\frac{1}{5}$, which is greater than $\frac{1}{6}$. For $M = 2$, we use two 5-sided code generators that independently and randomly produce $\mathbf{C}^{5 \times 5}$ quantization codes/codevectors. From this set, we select $\mathbf{C}^{5 \times 2}$ codes for consideration.

In this scenario, we observe that out of the 10 channel realizations, 8 codes are unique, while $2-c_{11}$ and c_{22} are identical. Consequently, we have $M_c'' < M'$, which aligns with Case 2 discussed earlier. Moreover, in this case, the codebook exhibits a non-unique code probability of $\frac{1}{5}$ and a unique code probability of $\frac{4}{5}$.

Therefore, when the non-unique code probability exceeds $\frac{1}{N}$, the AvgSysErr of the FRF MU-MIMO system will not align with that of the FRF MISO system.

Since both Assumption 1 and Assumption 2 do not hold, we proceed to examine **Lemma 1** by considering cases where the non-unique code probability of the generated codes is less than $\frac{1}{N}$.

Following a similar process from the previous assumptions, let's now consider the case where the non-unique code probability is $\frac{1}{7}$, which is less than $\frac{1}{6}$.

For $M = 2$, the process will independently and randomly generate $\mathbf{C}^{7 \times 7}$ quantization codes/codevectors. From this, we select $\mathbf{C}^{7 \times 2}$ codes for consideration. Although two codes, c_{11} and c_{22} , are identical out of 14 total codes, there are still 12 unique codes corresponding to 12 channel realizations. Thus, we have $M_c'' = M'$, which aligns with Case 1, as discussed earlier. Additionally, the codebook exhibits a non-unique code probability of $\frac{1}{7}$ and a unique code probability of $\frac{6}{7}$.

Therefore, when the non-unique code probability is less than $\frac{1}{N}$, the AvgSysErr of the FRF MU-MIMO system aligns with that of the FRF MISO system. As we continue to generate quantization codes/codevectors for systems like 8×2 , 9×2 , and so on—considering non-unique code probabilities of $\frac{1}{8}$ and $\frac{1}{9}$, respectively—these scenarios resemble Case 3, where $M_c'' > M'$.

Mathematically, when $M_c'' > M'$, the AvgSysErr no longer aligns with that of the MISO system, as the CQE decreases. However, from a practical standpoint, since there are sufficient unique codes generated to match the one-to-one channel realizations, the AvgSysErr effectively aligns. Case 3 simply indicates that there are more unique quantization codes/codevectors available in the codebook for channel quantization.

The summary of the $P(\text{Non_Uniq}, M')$, the case scenarios, and the AvgSysErr of the considered $N \times M'$ system is presented in Table 1 on top of the next page. We conclude that for FRF MU-MIMO systems, the AvgSysErr is conserved with the MISO system when the non-unique code probability of the generated codebook is always less than $\frac{1}{N}$.

In the example above with 6×2 system, the $P(\text{Non_Uniq}, 2) = \frac{1}{7}$ and less conserves the AvgSysErr with MISO system, since we know $\frac{1}{5} > \frac{1}{6} > \frac{1}{7} > \frac{1}{8} > \frac{1}{9}$. This general principle holds, where $\frac{1}{N_1} > \frac{1}{N_2} > \dots > \frac{1}{N_n}$, provided $N_1 < N_2 < \dots < N_n$.

However, the lower bound for the non-unique code probability remains unknown. In the following section, we address this lower bound with **Lemma 2**.

E. LOWER BOUND OF NON-UNIQUE CODE PROBABILITY

Lemma 2: The lower bound for the non-unique code probability of the generated quantization codes/codevectors, $P(\text{Non_Uniq}, N_n - N_{n-1})$, should be less than or equal to ε , where ε represents the difference between the non-unique code probabilities $\frac{1}{N_1}$ and $\frac{1}{N_2}$, given $\frac{1}{N_1} > \frac{1}{N_2}$. Specifically, $P(\text{Non_Uniq}, N_n - N_{n-1}) \leq \varepsilon$.

Proof: Consider the cases where $N = 6$, with $M = 3$ and $M = 4$, forming 6×3 and 6×4 systems, respectively. As part of the quantization code generation process, we use an N -sided unbiased code generator, where each receiver antenna is assigned a code. For $M = 3$ and $M = 4$, the process independently and randomly generates $6 \times 6 \times 6$ and $6 \times 6 \times 6 \times 6$ combinations of codes.

We know that using two identical combinations of codes for channel quantization increases the non-unique probability, leading to a rise in CQE. For both $M = 3$ and $M = 4$, we aim to calculate the non-unique probability of the quantization codes/codevectors as N increases and determine the lower bound with ε .

From **Lemma 1**, we established that the non-unique code probability should always be less than $\frac{1}{N}$. As N increases, we compare the change in the non-unique probability with ε . To confirm, we check whether any two identical quantization codes/codevectors occur in the generated codebook, which would contribute to the non-unique code probability. For $M = 3$ and $M = 4$, the probability of generating two identical codes when using three or four unbiased N -sided code generators (corresponding to $M = 3$ and $M = 4$ receiver antennas) at the APs, randomly and independently, is given by the following equations [33], [34]:

$$P(\text{Non_Uniq}, 3) = \frac{\binom{3}{2} \times N \times N - 1}{N^3} \quad (15)$$

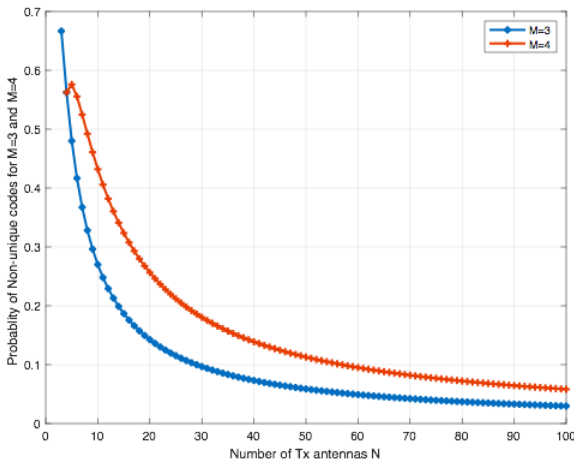
and

$$P(\text{Non_Uniq}, 4) = \frac{\binom{4}{2} \times N \times N - 1 \times N - 2}{N^4}. \quad (16)$$

We now calculate the non-unique probability of the generated quantization codebook as N increases. Figure 6 shows the curve representing the non-unique probability for an M -receiver antenna system, $P(\text{Non_Uniq}, M)$, where $M = 3$ and $M = 4$, as the number of transmitter antennas, N , increases. We observe that both $P(\text{Non_Uniq}, 3)$ and $P(\text{Non_Uniq}, 4)$ decrease with increasing N , and the curve asymptotically approaches the x-axis.

TABLE 1. Summary of the $P(\text{Non_Uniq}, M')$, the case scenarios and the AvgSysErr of the considered $N \times M'$ system.

System	Non-unique code probability of the Codebook $P(\text{Non_Uniq})$	Case Scenario	AvgSysErr
$N \times M'$	$P(\text{Non_Uniq}, M') = \frac{1}{N}$	Case 1, i.e., $M_c'' < M'$	Not Conserved with MISO
	$P(\text{Non_Uniq}, M') > \frac{1}{N}$	Case 1, i.e., $M_c'' < M'$	Not Conserved with MISO
	$P(\text{Non_Uniq}, M') < \frac{1}{N}$	Case 2, i.e., $M_c'' = M'$ when, $P(\text{Non_Uniq}, M') = \frac{1}{N+i}$, where $i=1$.	Conserved with MISO
		Case 3, i.e., $M_c'' > M'$ when, $P(\text{Non_Uniq}, M') < \frac{1}{N+j}$, where $j=2,3,\dots,n$.	

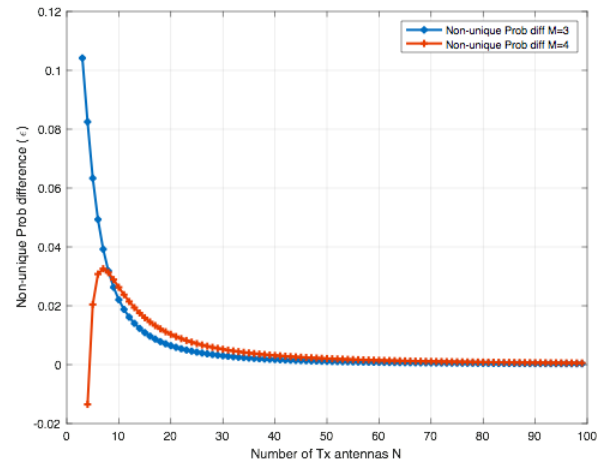
**FIGURE 6.** Non-unique probability vs N .

The decrement in $P(\text{Non_Uniq}, 3)$ and $P(\text{Non_Uniq}, 4)$ as N increases, is expected since the quantization codebook expands as more transmitter antennas are added, effectively creating a taller codebook. This provides more unique codes for channel quantization, particularly for $M = 3$ and $M = 4$. As a result, $P(\text{Uniq}, M) = 1 - P(\text{Non_Uniq}, M)$ increases with N . Since $(M = 4) > (M = 3)$, the non-unique probability $P(\text{Non_Uniq}, 4)$ is slightly greater than $P(\text{Non_Uniq}, 3)$, as illustrated in Figure 6. This is because there is a higher likelihood of generating two identical codes when the number of receiver antennas $M = 4$ exceeds $M = 3$.

The $P(\text{Non_Uniq}, M)$ vs N curve also indicates that as N increases, $P(\text{Non_Uniq}, M)$ approaches saturation, meaning there is no significant change in the non-unique probability as N continues to grow. This suggests that the lower bound for $P(\text{Non_Uniq}, M)$ can be reached.

The asymptotic behaviour of $P(\text{Non_Uniq}, M)$ relative to the x-axis is justified by the fact that some degree of code repetition is inevitable, regardless of how tall the codebook becomes with increasing N . This is due to the random, independent, and distributed generation of quantization codes/codevectors at each AP.

In other words, the asymptotic nature of the curve reflects the reality that, regardless of how large the codebook N^M

**FIGURE 7.** ε vs N .

grows, at least two identical codes are likely to exist. This arises from the inherent randomness in the codebook generation process. Figure 7 depicts the curve of ε versus N , where ε represents the difference in the non-unique probability between N_n and N_{n-1} . The asymptotic nature of this curve suggests that the difference in non-unique probabilities, ε , saturates as N increases. A small value for ε can be set based on the specific requirements of the SC system under consideration. Thus, the non-unique probability, $P(\text{Non_Uniq}, N_n - N_{n-1})$, can be controlled to be less than or equal to ε , ensuring that no further changes in $P(\text{Non_Uniq}, N_n - N_{n-1})$ occur, even as N continues to grow. This behaviour helps to illustrate the lower bound of $P(\text{Non_Uniq}, M)$.

It is important to note that $P(\text{Non_Uniq}, N_n - N_{n-1}) \leq \varepsilon$ holds true for any number of receiver antennas, i.e., $M = 1, 2, 3, \dots, n$, in the case of SC systems. This is because, regardless of how much we increase N or M , the non-unique probability $P(\text{Non_Uniq}, M)$ will remain asymptotic to the x-axis for each incremental increase in M . This behaviour results from the inherent probability of generating identical outcomes when using two independent, N -sided unbiased code generators. Therefore, **Lemma 2** can be generalized to any M and N , ensuring that the relationship between the

non-unique probability and ε holds universally across all configurations of transmitter and receiver antennas. \square

V. CONCLUSION

In the context of dynamic, distributive, and densely deployed SCs aimed at enhancing system coverage, capacity, and QoS, we have examined the adaptive and distributed per-receiver antenna quantization approach. To maintain control over the CQE and AvgSysErr, the threshold for the non-unique code probability in the per-receiver antenna quantization codebook was identified as being less than $\frac{1}{N}$, where N is the number of transmitter antennas at the APs. Additionally, the lower bound for the non-unique code probability was established as being less than ε , a small, customisable design parameter for SC systems.

While the proposed per-antenna quantization approach has been evaluated in reference to the MISO system, the underlying framework is extendable to MIMO configurations, which are increasingly relevant in heterogeneous and dense small cell deployments. As modern user equipment evolves to support multiple antennas, future work will focus on implementing and analyzing the proposed method in a full MU-MIMO system. This will allow for a more comprehensive understanding of its performance under joint receiver-side processing and spatial multiplexing, and will further demonstrate its scalability and robustness in practical network scenarios.

In addition, it would be valuable to explore the impact of quantization code mismatches on CQE. Such mismatches, which violate the 1:1 mapping between channel realizations and quantization codes/codevectors, present a significant risk in limited feedback systems and warrant deeper investigation. We envision that with the full-fledged 6G and IoT implementations, the deployment of SCs will be ubiquitous for system coverage, capacity and QoS. In such a context, interference management could be one of the challenging aspects of SCs deployment, which is partly discussed in [36]. Further, the distributed nature of the per-receiver antenna-based quantization can be envisioned inline with the concept of edge computing, where the promising federated learning (FL) approach could be used to train the model for finding out more non-unique codes for quantization for the SCs, which may help avoiding the increment of the CQE and AvgSysErr.

REFERENCES

- [1] *5G Technology & Small Cells*. (2024). Accessed: Oct. 10, 2024. [Online]. Available: <https://www.infrastructure.gov.au/departments/media/news/5g-technology-small-cells>
- [2] A. Adel, "Future of industry 5.0 in society: Human-centric solutions, challenges and prospective research areas," *J. Cloud Comput.*, vol. 11, no. 1, pp. 1–15, Sep. 2022.
- [3] *About small cells*. Accessed: Oct. 10, 2024. [Online]. Available: <https://www.smallcellforum.org/small-cells>
- [4] *Small cells a major game changer*. Accessed: Oct. 10, 2024. [Online]. Available: <https://telecom.com/en/small-cells-a-major-game-changer/>
- [5] *Small cells*. Accessed: Oct. 10, 2024. [Online]. Available: <https://www.ericsson.com/en/small-cells>
- [6] *Small cells—Focused coverage and optimum performance*(2024). Accessed: Oct. 10, 2024. [Online]. Available: <https://www.nokia.com/networks/mobile-networks/small-cells/>
- [7] *Small Cell 5G Network Market*. Accessed: Oct. 10, 2024. [Online]. Available: <https://www.factmr.com/report/small-cell-5g-network-market>
- [8] D. J. Love, R. W. Heath, and T. Strohmer, "Grassmannian beamforming for multiple-input multiple-output wireless systems," *IEEE Trans. Inf. Theory*, vol. 49, no. 10, pp. 2735–2747, Oct. 2003.
- [9] K. K. Mukkavilli, A. Sabharwal, E. Erkip, and B. Aazhang, "On beamforming with finite rate feedback in multiple-antenna systems," *IEEE Trans. Inf. Theory*, vol. 49, no. 10, pp. 2562–2579, Oct. 2003.
- [10] A. Narula, M. J. Lopez, M. D. Trott, and G. W. Wornell, "Efficient use of side information in multiple-antenna data transmission over fading channels," *IEEE J. Sel. Areas Commun.*, vol. 16, no. 8, pp. 1423–1436, 1998.
- [11] D. J. Love, R. W. Heath Jr., W. Santipach, and M. L. Honig, "What is the value of limited feedback for MIMO channels?" *IEEE Commun. Mag.*, vol. 42, no. 10, pp. 54–59, Oct. 2004.
- [12] C. Au-Yeung and D. Love, "On the performance of random vector quantization limited feedback beamforming in a MISO system," *IEEE Trans. Wireless Commun.*, vol. 6, no. 2, pp. 458–462, Feb. 2007.
- [13] N. Jindal, "MIMO broadcast channels with finite-rate feedback," *IEEE Trans. Inf. Theory*, vol. 52, no. 11, pp. 5045–5060, Nov. 2006.
- [14] T. Yoo, N. Jindal, and A. Goldsmith, "Multi-antenna downlink channels with limited feedback and user selection," *IEEE J. Sel. Areas Commun.*, vol. 25, no. 7, pp. 1478–1491, Sep. 2007.
- [15] P. Ding, D. J. Love, and M. D. Zoltowski, "On the sum rate of channel subspace feedback for multi-antenna broadcast channels," in *Proc. IEEE Global Telecommun. Conf.*, Nov. 2005, pp. 1–5.
- [16] M. Sharif and B. Hassibi, "On the capacity of MIMO broadcast channels with partial side information," *IEEE Trans. Inf. Theory*, vol. 51, no. 2, pp. 506–522, Jan. 2005.
- [17] K. Huang, J. G. Andrews, and R. W. Heath Jr., "Performance of orthogonal beamforming for SDMA with limited feedback," *IEEE Trans. Veh. Technol.*, vol. 58, no. 1, pp. 152–164, Jan. 2006.
- [18] D. Love, R. Heath, V. N. Lau, D. Gesbert, B. Rao, and M. Andrews, "An overview of limited feedback in wireless communication systems," *IEEE J. Sel. Areas Commun.*, vol. 26, no. 8, pp. 1341–1365, Oct. 2008.
- [19] J. Mo and R. W. Heath Jr., "Limited feedback in single and multi-user MIMO systems with finite-bit ADCs," *IEEE Trans. Wireless Commun.*, vol. 17, no. 5, pp. 3284–3297, May 2018.
- [20] P. Ding, D. J. Love, and M. D. Zoltowski, "Multiple antenna broadcast channels with shape feedback and limited feedback," *IEEE Trans. Signal Process.*, vol. 55, no. 7, pp. 3417–3428, Jul. 2007.
- [21] N. Ravindran and N. Jindal, "Multi-user diversity vs. Accurate channel state information in MIMO downlink channels," *IEEE Trans. Wireless Commun.*, vol. 11, no. 9, pp. 3037–3046, Sep. 2012.
- [22] F. Kaltenberger, M. Kountouris, D. Gesbert, and R. Knopp, "On the trade-off between feedback and capacity in measured MU-MIMO channels," *IEEE Trans. Wireless Commun.*, vol. 8, no. 9, pp. 4866–4875, Sep. 2009.
- [23] X. Shang, B. Chen, and H. V. Poor, "Multiuser MISO interference channels with single-user detection: Optimality of beamforming and the achievable rate region," *IEEE Trans. Inf. Theory*, vol. 57, no. 7, pp. 4255–4273, Jul. 2011.
- [24] S. W. Choi, W.-Y. Shin, and J. Kim, "Linear algebraic beamforming design for multiuser MISO interference channels: A reduction in search space dimension," *Entropy*, vol. 20, no. 6, p. 431, Jun. 2018.
- [25] X. Shang, B. Chen, and M. J. Gans, "On the achievable sum rate for MIMO interference channels," *IEEE Trans. Inf. Theory*, vol. 52, no. 9, pp. 4313–4320, Sep. 2006.
- [26] R. Zhang and S. Cui, "Cooperative interference management with MISO beamforming," *IEEE Trans. Signal Process.*, vol. 58, no. 10, pp. 5450–5458, Oct. 2010.
- [27] R. Zhang, "Cooperative multi-cell block diagonalization with per-base-station power constraints," *IEEE J. Sel. Areas Commun.*, vol. 28, no. 9, pp. 1435–1445, Dec. 2010.
- [28] A. Carleial, "A case where interference does not reduce capacity (corresp.)," *IEEE Trans. Inf. Theory*, vol. IT-21, no. 5, pp. 569–570, Sep. 1975.
- [29] X. Shang, B. Chen, G. Kramer, and H. V. Poor, "Capacity regions and sum-rate capacities of vector Gaussian interference channels," *IEEE Trans. Inf. Theory*, vol. 56, no. 10, pp. 5030–5044, Oct. 2010.
- [30] G. Lee, J. Park, Y. Sung, and M. Yukawa, "Coordinated beamforming with relaxed zero forcing," in *Proc. Int. Conf. Wireless Commun. Signal Process. (WCSP)*, Nov. 2011, pp. 1–5.

- [31] S. Shrestha, "Addressing the hidden terminal problem in MU-MIMO w lans with relaxed zero-forcing approach," Ph.D. dissertation, School Comput. Commun., Univ. Technol. Sydney, Australia, 2017.
- [32] S. Shrestha, G. Fang, E. Dutkiewicz, and X. Huang, "Effect of CSI quantization on the average rate in MU-MIMO WLANs," in *Proc. 13th IEEE Annu. Consum. Commun. Netw. Conf. (CCNC)*, Jan. 2016, pp. 824–828.
- [33] J. L. Devore, *Probability and Statistics for Engineering and the Sciences*. London, U.K.: Duxbury Press, 2000.
- [34] R. E. Walpole, R. H. Myers, S. L. Myers, and K. Ye, *Probability and Statistics for Engineers and Scientists*, vol. 5. New York, NY, USA: MacMillan, 1993.
- [35] S. Shrestha, B. Bhandari, and S. Bevinakoppa, "Distributive quantization codes for finite rate feedback-based small cells," in *Proc. IEEE 22nd Consum. Commun. Netw. Conf. (CCNC)*, Jan. 2025, pp. 1–6.
- [36] S. Shrestha, X. Huang, K. Saleem, S. Bevinakoppa, and T. Jan, "Quantification of interference constraint for small cells in low SINR regime with steepest ascent method," *IEEE Access*, vol. 13, pp. 2328–2339, 2025.
- [37] E. Koyuncu and H. Jafarkhani, "Variable-length limited feedback beamforming in multiple-antenna fading channels," *IEEE Trans. Inf. Theory*, vol. 60, no. 11, pp. 7140–7165, Nov. 2014.



SANJEEB SHRESTHA received the bachelor's degree in electronics and communication from Kantipur City College, Purbanchal University, Nepal, in 2008, the master's degree in information and communication systems from Harbin Engineering University, China, in 2012, and the Ph.D. degree in wireless communication from the University of Technology Sydney (UTS), in 2017. He is a Lecturer with SITE, Melbourne Institute of Technology, Sydney Campus. His research interests include addressing long-standing problems in wireless communications, such as interference constraints in MIMO, hidden terminal problems, and rate and capacity regions. Lately, he has also been interested in the IoT systems, cybersecurity, machine learning, deep learning, artificial intelligence (AI), and educational research, such as score standardization, GenAI usage, and analysis.



XIAOYING KONG received the Bachelor of Engineering and Master of Engineering degrees in control engineering from Beijing University of Aeronautics and Astronautics, in 1986 and 1989, respectively, and the Ph.D. degree in mechatronic engineering from The University of Sydney, in 2000. She is currently a Senior Lecturer with Melbourne Institute of Technology. She has many years' work experience in aeronautical industry, semiconductor industry, and software industry. Her research interests include control engineering and software engineering. She has published research articles broadly on software engineering, data engineering, inertial navigation systems, GPS, sensor fusion, positioning sensor networks, vehicle navigation, and path control.



PAUL KWAN (Senior Member, IEEE) received the B.Sc. degree in computer science from Cornell University, New York, USA, in 1986, the M.Sc. degree in computer science from The University of Arizona, Arizona, USA, in 1988, and the Ph.D. degree in advanced engineering systems, majoring in intelligent interaction technologies from the University of Tsukuba, Japan, in 2003.

He is currently an Associate Professor of ICT with the School of Engineering and Technology (SET), CQUniversity Australia, Brisbane Campus. His research interests include artificial intelligence and data science. Within these fields, his expertise includes computer vision, data mining, machine learning, and computational modeling. His expertise has informed applied research in image retrieval, biometrics authentication, dimensionality reduction, agent-based modeling, digital agriculture, and learning analytics. To date, he has published over 120 peer-reviewed papers and refereed articles in international conferences and journals in *Artificial Intelligence*, *Computer Vision*, *Pattern Recognition*, *Digital Agriculture*, and *Education Sciences*.



XIAOJING HUANG (Senior Member, IEEE) received the B.Eng., M.Eng., and Ph.D. degrees in electronic engineering from Shanghai Jiao Tong University, Shanghai, China, in 1983, 1986, and 1989, respectively. He was a Principal Research Engineer with the Motorola Australian Research Center, Botany, NSW, Australia, from 1998 to 2003, and an Associate Professor with the University of Wollongong, Wollongong, NSW, from 2004 to 2008. He has been a Principal Research Scientist with the Commonwealth Scientific and Industrial Research Organisation (CSIRO), Sydney, NSW, and the Project Leader of the CSIRO Microwave and mm-Wave Backhaul projects, since 2009. He is currently a Professor of information and communications technology and the Head of the Electronics and Communications Discipline, School of Electrical and Data Engineering, University of Technology Sydney (UTS), Sydney, NSW. With over 36 years of combined industrial, academic, and scientific research experience, he has authored over 450 book chapters, refereed journal and conference papers, major commercial research reports, and filed 31 patents. His research interests include high-speed wireless communications, digital and analog signal processing, and synthetic aperture radar imaging. He was a recipient of the CSIRO Chairman's Medal and Australian Engineering Innovation Award in 2012 for exceptional research achievements in multigigabit wireless communications.

...